

## Supplementary Information

### The Neuromelanin-related T<sub>2</sub>\* Contrast in Postmortem Human Substantia Nigra with 7T MRI

Jae-Hyeok Lee <sup>a,1</sup>, Sun-Yong Baek <sup>b,1</sup>, YoungKyu Song <sup>c</sup>, Sujeong Lim <sup>c</sup>, Hansol Lee <sup>c</sup>, Minh Phuong Nguyen <sup>d</sup>, Eun-Joo Kim <sup>e</sup>, Gi Yeong Huh <sup>f</sup>, Se Young Chun <sup>d,\*</sup>, HyungJoon Cho <sup>c,\*</sup>

<sup>a</sup> Department of Neurology, Research Institute for Convergence of Biomedical Science and Technology, Pusan National University Yangsan Hospital, Yangsan, South Korea

<sup>b</sup> Department of Anatomy, Pusan National University School of Medicine, Yangsan, South Korea

<sup>c</sup> Department of Biomedical Engineering, Ulsan National Institute of Science and Technology, Ulsan, South Korea

<sup>d</sup> School of Electrical and Computer Engineering, Ulsan National Institute of Science and Technology, Ulsan, South Korea

<sup>e</sup> Department of Neurology, Pusan National University Hospital, Busan, South Korea

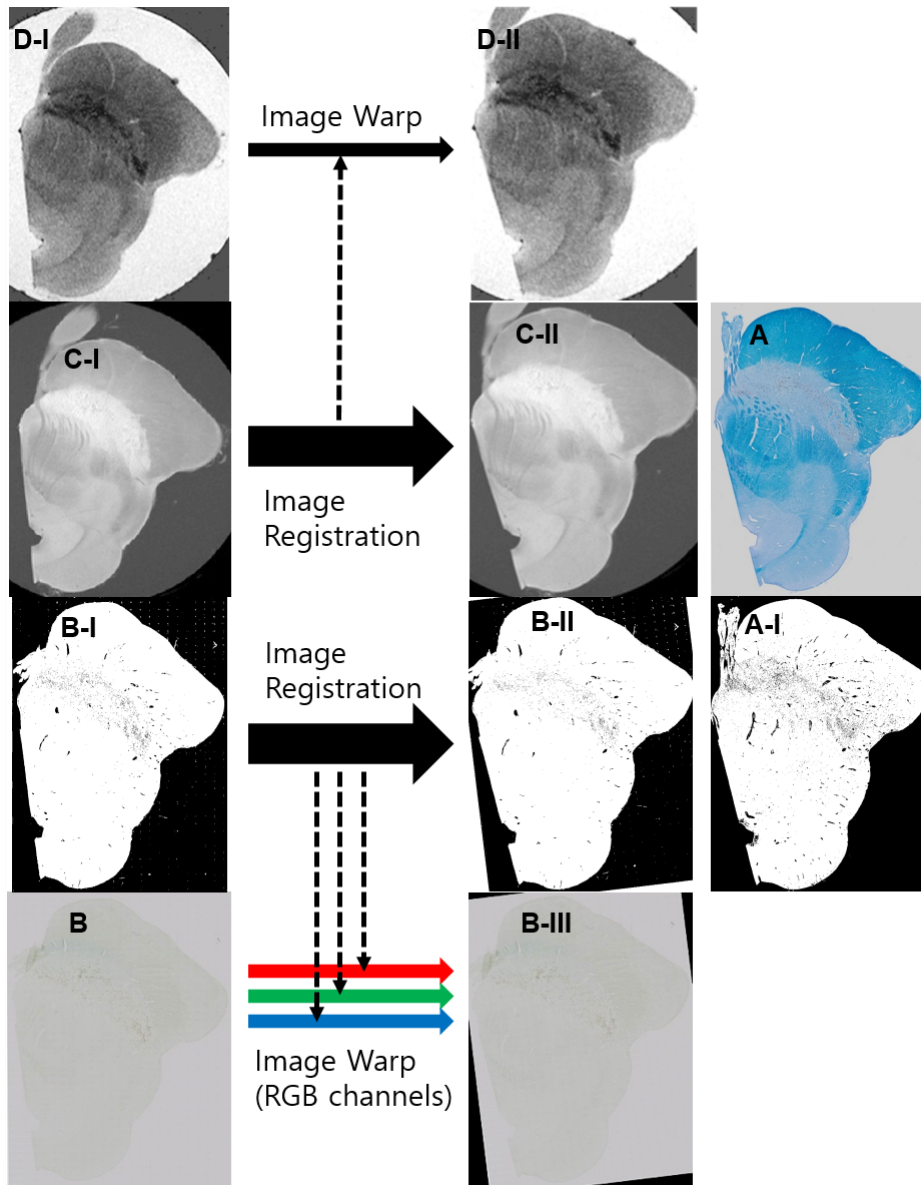
<sup>f</sup> Department of Forensic Medicine, Pusan National University School of Medicine, Yangsan, South Korea

<sup>1</sup> Co-first authors.

\* Corresponding authors.

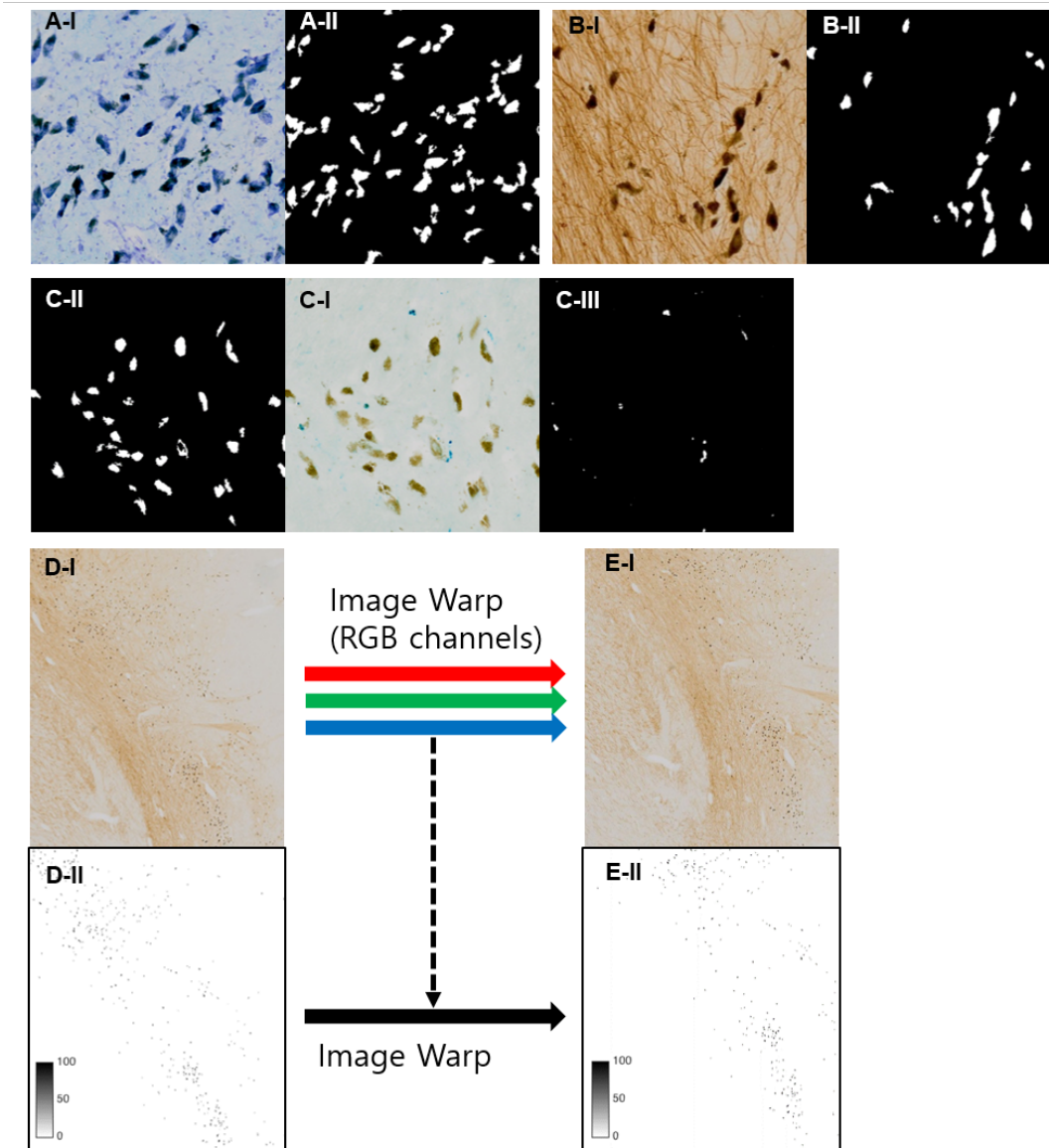
E-mail addresses: [sychun@unist.ac.kr](mailto:sychun@unist.ac.kr) (S.Y.C.), [hjcho@unist.ac.kr](mailto:hjcho@unist.ac.kr) (H.J.C.).

## Supplementary Figure S1



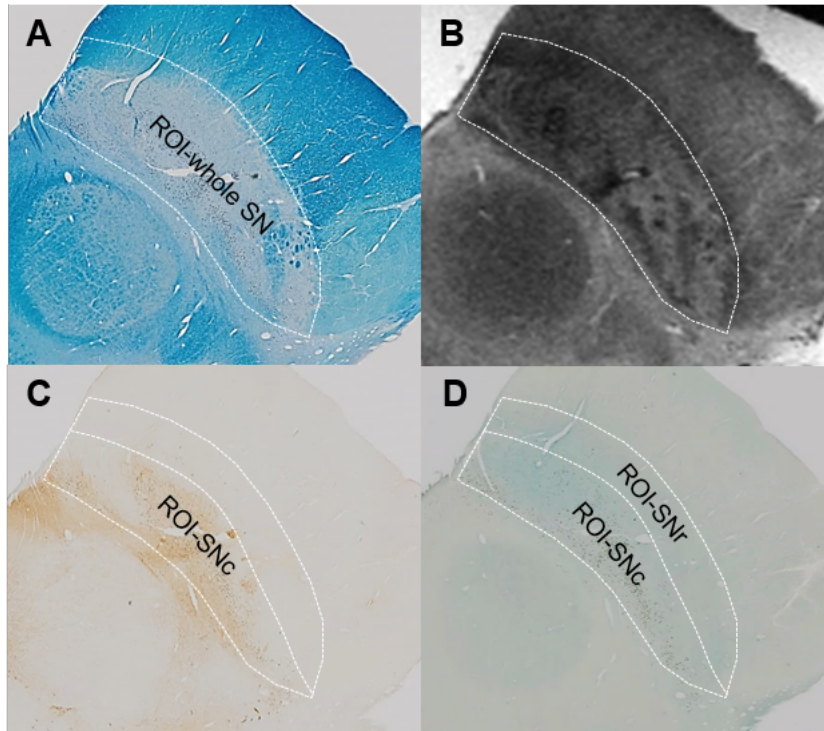
**Supplementary Figure S1.** The schematic diagram of the histology-MRI image registration. The binary Perl image (B-I) (from the Perl stain image (B)) was registered to the binary KB image (A-I) (from the KB stain image (A)) to yield an aligned binary Perl image (B-II). Then, the resulting transformation information was used to warp the RGB channel information from the original Perl stain image (B) to generate the aligned Perl stain image (B-III). The original  $T_1$ WI (C-I) was registered to the KB stain image (A) using red channel information, to yield the aligned  $T_1$ WI (C-II). The same transformation information was used to warp the original  $T_2^*$ WI (D-I) to the registered  $T_2^*$ WI (D-II).

## Supplementary Figure S2



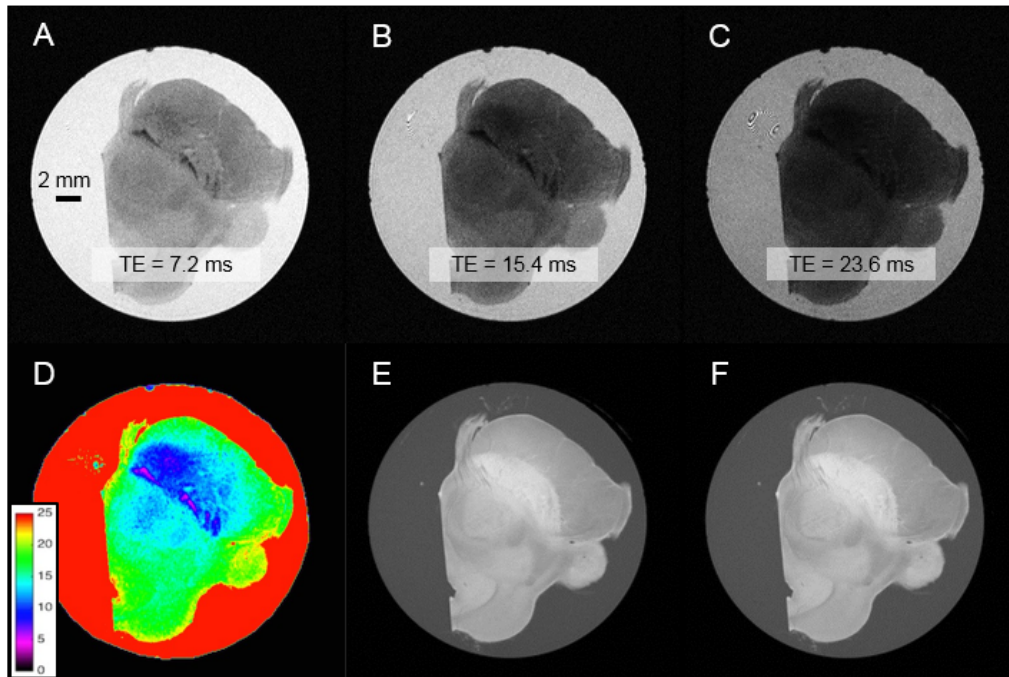
**Supplementary Figure S2.** Neuron-occupied areas (A-II and B-II) were extracted from 2D KB (A-I) and TH (B-I) stained images. Iron pigments (C-III) and unstained pigmented NM (C-II) were also extracted from 2D Perl stained images (C-I, the same two figures) to obtain iron and NM density maps. Then, the number of pixels occupied by neurons or pigments per 10×10 block was recorded to generate a density map (% occupied by neurons) as shown in D-II (only TH case shown). Then, the TH-positive neuron density image (D-II) ranging from 0 to 100% was registered to the closest KB stain image to yield the aligned density image (E-II) using the same transformation information to warp from the original TH stain image (D-I) to the aligned image (E-I).

### Supplementary Figure S3



**Supplementary Figure S3.** The polygonal regions of interest (ROIs). ROI-whole SN (A) based on the KB stain corresponding to the most of SN hypointensity on the T<sub>2</sub>\*WI (B), ROI-SNc (the substantia nigra pars compacta) based on the TH stain within the ROI-whole SN including the A9 cell group (C), and ROI-SNr (the substantia nigra pars reticulata) obtained by subtracting ROI-SNc from ROI-whole SN (D).

### Supplementary Figure S4



**Supplementary Figure S4.** The ex vivo substantia nigra MRI protocol (70-year-old female subject, at the rostral level the exiting third cranial nerve fibers). For the  $T_2^*$ WI, an echo time of TE = 15.4 ms yielded the best visual MRI contrast among the ten different TEs, ranging from 3.1 to 40 ms (A, B, C). For the color-coded  $T_2^*$  map (D), the color bar represents  $T_2^*$  values (ms). The  $T_1$ WI (E) presents arch-shaped boundaries between the SN and the crus cerebri more distinctly than  $T_2^*$ WI. The magnetization transfer  $T_1$ -weighted image (F) is unable to accurately depict NM-related contrasts in the substantia nigra pars compacta.

### Supplementary Table S1

Multiple R	Subject I	Subject II
T <sub>2</sub> * with Iron	0.49	0.31
T <sub>2</sub> * with Iron, NM	0.56	0.70
T <sub>2</sub> * with Iron, NM, Nissl	0.56	0.70
T <sub>2</sub> * with Iron, NM, Nissl, TH	0.58	0.71

**Supplementary Table S1.** Coefficients of multiple correlation (multiple R) for T<sub>2</sub>\* with histologic measures such as iron, NM, Nissl, and TH. These show that Nissl and TH are almost co-linear with NM and Iron since adding Nissl and TH to linear models did not increase multiple R much.

### Supplementary Table S2

Pearson's Correlation (Spearman's Correlation)	Nissl	TH	NM
Subject I (six slices)			
TH	0.59* (0.68*)		
NM	0.82* (0.82*)	0.62* (0.66*)	
Iron	0.07 (0.30*)	0.01 (0.19*)	0.05 (0.30*)
Subject II (six slices)			
TH	0.69* (0.77*)		
NM	0.85* (0.86*)	0.69* (0.75*)	
Iron	-0.27* (-0.33*)	-0.17* (-0.12**)	-0.25* (-0.27*)

TH: tyrosine hydroxylase, NM: neuromelanin. \*  $P < 0.0001$ , \*\*  $P < 0.005$

**Supplementary Table S2.** Pearson's correlations (Spearman's correlations in parentheses) between the densities of the histological components.